Available online at www.eccomasproceedia.org
Eccomas Proceedia COMPDYN (2023) 994-1004

ECCOMAS
Proceedia

COMPDYN 2023
9th ECCOMAS Thematic Conference on
Computational Methods in Structural Dynamics and Earthquake Engineering
M. Papadrakakis, M. Fragiadakis (eds.)
Athens, Greece, 12-14 June 2023

EXPERIMENTAL STUDY OF PHONONIC STRUCTURES WITH DDA ENHANCED UNIT-CELLS

M. Kalderon [1], A. Mantakas [2], K.A. Chondrogiannis [3], I.A. Antoniadis [1]

[1] National Technical University of Athens, School of Mechanical Engineering, Department of Mechanical Design & Automatic Control, Dynamics & Acoustics Laboratory
Heroon Polytechniou 9, 15780 Zografou, Athens, Greece
moriska@mail.ntua.gr, antogian@central.ntua.gr

[2] National Technical University of Athens, School of Civil Engineering, Department of Structural Engineering, Institute of Structural Analysis and Antiseismic Research
Heroon Polytechniou 9, 15780 Zografou, Athens, Greece
mantakasantonis@gmail.com

[3] ETH Zurich, Department of Civil, Environmental and Geomatic Engineering
Stefano-Franscini-Platz 5, Zurich 8093, Switzerland
Chondrogiannis@ibk.baug.ethz.ch

Abstract

Phononic structures with periodic unit-cells that exhibit Bragg scattering, have been investigated during the latest years by various researchers due to their extraordinary wave manipulation and filtering properties. One major feature of these metamaterials is their ability to generate stopbands or bandgaps in the frequency domain, hence presenting significant vibration attenuation properties. However, this mechanism presents certain design constraints in generating broadband bandgaps, especially in the low-frequency range, where large masses are required. To this end, a novel dynamic directional amplifier, namely the DDA, is introduced as a means to artificially increase the inertia of an oscillating mass. The DDA is realized by imposing kinematic constraints to the degrees of freedom (DoFs) of the oscillator, hence inertia is increased by coupling the horizontal and vertical motion. In this study, the DDA is implemented in an experimental scaled phononic set-up that is constructed using LEGO® Technic components. Experimental testing is undertaken as a feasibility assessment of the concept and results indicate the low-frequency wave attenuation properties of the structure.

Keywords: Phononic structures, Metamaterials, Amplification mechanism, Experiment, Vibration control.

ISSN:2623-3347
Peer-review under responsibility of the organizing committee of COMPDYN 2023.
doi: 10.7712/120123.10452.20430

1 INTRODUCTION

Phononic structures with unit-cells exhibiting Bragg scattering present unique wave propagation properties at wavelengths well below the regime corresponding to bandgap generation based on spatial periodicity. Thus, to have a low-frequency Bragg gap, low wave speeds i.e., large lattice constant are required, while heaviness, low stiffness, and large size prohibit their exploitation in practical purposes [1].

Therefore, achieving wide and low-frequency bandgaps, based solely on conventional phononic structures is a challenge. Recent attempts have been made towards artificially increasing the resonating mass's inertia via amplification mechanisms. Inspired by the successful application of inertial amplifiers in engineering applications, several works proved their suitability in the context of periodic structures [2–6]. Several architected metamaterial structures with inertial amplification mechanisms [7–9] or negative stiffness properties [10,11] have been manufactured and experimentally tested. Yilmaz and his research team [2,4,12–14] first introduced designs of periodic structures with embedded inertial amplification mechanisms and conducted a series of experiments in compliant periodic structures, 3D printed specimens, as well as samples manufactured by aluminum beams. Similarly, Bergamini et al. [15] and Zaccherini et al. [16] exploited chirality and tested 3D printed elements searching for large low-frequency bandgaps, while Chondrogiannis et al. [17] examined a geometrically nonlinear metamaterial constructed by LEGO® Technic bricks.

In this paper, inspired by the benefits induced by the insertion of DDA mechanisms within the structure [18–21], one-dimensional inertial amplified lattices are designed for the mitigation of low-frequency mechanical vibrations. To this end, a DDA-enhanced phononic metamaterial chain is constructed and tested, consisting of LEGO® Technic bricks. Results validate the concept of DDA-enhanced structures and prove that the proposed metamaterials can be adequately described by the developed analytical and numerical models. Lastly, the established prototypes indicate that realistic full-scale designs are feasible and suitable for a wide range of applications, i.e., seismic mitigation, vibration isolation, acoustic mitigation etc.

2 THEORETICAL BACKGROUND

2.1 The Dynamic Directional Amplification (DDA) mechanism

The Cartesian coordinate system is established as shown in Figure 1. Connecting the mass to the origin of the local coordinate system (CSYS) via a hinged, rigid rod of length AB=L which is assumed to be massless for the purpose of this analysis, imposes a kinematic constraint between the DoFs u and v. The lumped parameter model is described by the coordinates of the mass (m) at a generic position B(x, y)=(x_0+u, y_0−v), where x_0, y_0 are the initial coordinates of the mass. The initial angle between the horizontal axis and the link is denoted by $\varphi = arctan(x_0 / y_0)$, while θ denotes the rotation of the rod at the generic position B of the moving mass. k_x, k_y are the springs stiffnesses, c_x, c_y the damping coefficients on the horizontal and vertical directions respectively, and F the force exciting the mass in the x direction.

The governing equation of the DDA mechanism in the direction of motion is given as follows:

$$M\ddot{u} + C\dot{u} + Ku = F \tag{1}$$

where, $M = (1 + tan^2(\varphi))m$, $C = c_x + c_y tan^2(\varphi)$ and $K = k_x + k_y tan^2(\varphi)$.

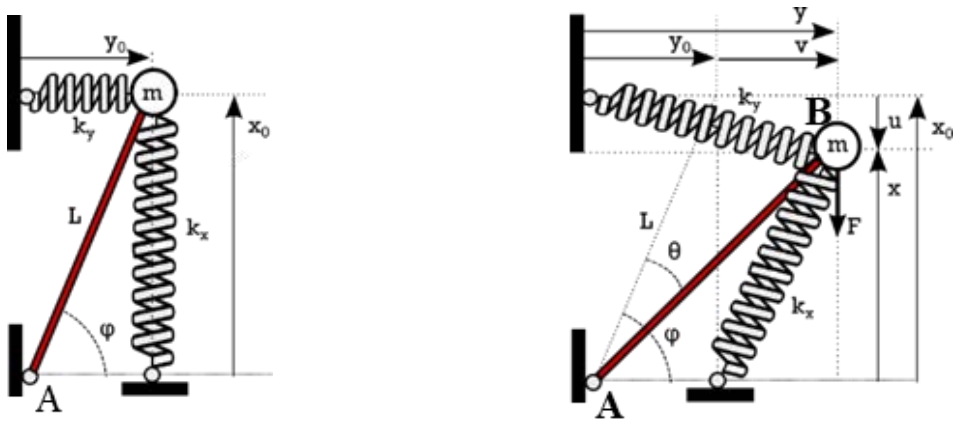

(a) (b)

Figure 1: Kinematic model of the Dynamic directional amplification (DDA) mechanism, where the motion v of mass m is kinematically constrained to the motion u, (a) initial mass position (b) mass position at deformed state.

2.2 2D phononic lattice with Dynamic Directional Amplification (DDA) mechanisms

The infinite mass–spring–dashpot lattice with the DDA is depicted in Figure 2.

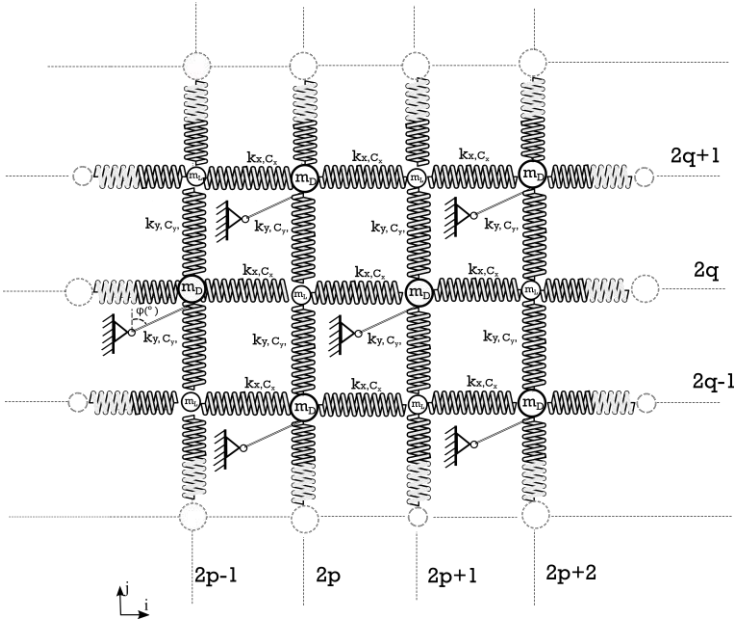

Figure 2: 2D phononic lattice with dynamic directional amplifiers (DDA).

Considering the case of the lattice under harmonic excitation the relative motion of the structural nodes will cause amplified motion for the masses m_D generating amplified inertial forces. Then, the wave propagation characteristics of this lattice are determined from the irreducible unit-cell via Bloch's theorem. The dispersion relationship of the phononic structure with directional inertial amplifiers is given by:

$$\det\left[-\lambda^2 \boldsymbol{M}_p \ddot{\boldsymbol{u}} + \lambda \boldsymbol{C}_P \dot{\boldsymbol{u}} + \boldsymbol{K}_P \boldsymbol{u}\right] = 0 \tag{2}$$

where

$$\boldsymbol{M}_{p,\alpha}=\begin{bmatrix} m_L & 0 & 0 \\ 0 & m_L & 0 \\ 0 & 0 & m_D(1+\rho^2) \end{bmatrix}$$

$$\boldsymbol{K}_{p,a}=\begin{bmatrix} 2k_x & 0 & -k_x(1+e^{-j\mu_x}) \\ 0 & 2k_y & 2\rho k_y e^{\frac{-j\mu_x}{2}}\cos\left(\frac{\mu_y}{2}\right) \\ -k_x\left(1+e^{j\mu_x}\right) & 2\rho k_y e^{\frac{j\mu_x}{2}}\cos\left(\frac{\mu_y}{2}\right) & 2k_x+2\rho^2 k_y \end{bmatrix} \tag{3}$$

$$\boldsymbol{C}_{p,a}=\begin{bmatrix} 2c_x & 0 & -c_x(1+e^{-j\mu_x}) \\ 0 & 2c_y & 2\rho c_y e^{\frac{-j\mu_x}{2}}\cos\left(\frac{\mu_y}{2}\right) \\ -c_x\left(1+e^{j\mu_x}\right) & 2\rho c_y e^{\frac{j\mu_x}{2}}\cos\left(\frac{\mu_y}{2}\right) & 2c_x+2\rho^2 c_y \end{bmatrix}$$

3 DESIGN OF THE EXPERIMENTAL DEVICE

Figure 3 depicts the conceptual LEGO® configuration where the amplifier is installed at the base of mass m_D. Apart from the extension springs that are custom made and the longitudinal guides that are made of aluminum to increase vertical and lateral rigidity, the metamaterial's components are assembled using LEGO® Technic parts. The selection of a LEGO® Technic assembly is adopted due to the design simplicity, cost, and accuracy merits compared to alternatives such as steel structures and 3D printed elements. The studied device was initially conceptualized and then drawn in Lego Digital Designer where different arrangements can be easily examined before assembling the actual physical models. The structure consists of only four (4) unit-cells, as per previous studies on various linear and nonlinear metamaterial designs [17,22,23] is shown that even for a reduced number of unit-cells a substantial bandgap can be generated, leading to noticeable motion reduction. A hinged connection is realized using the LEGO® Technic parts and allows the link to rotate freely, while a fixed base is built to support independently the DDA mechanisms. The unit-cells are connected by an arrangement of springs. To ensure that these springs work properly in both compression and extension, two additional coils of stiffness $k_e/2$ are installed to the LEGO® linear spring of stiffness k_c to keep the latter in a prestressed state [17], as illustrated in Figure 4.

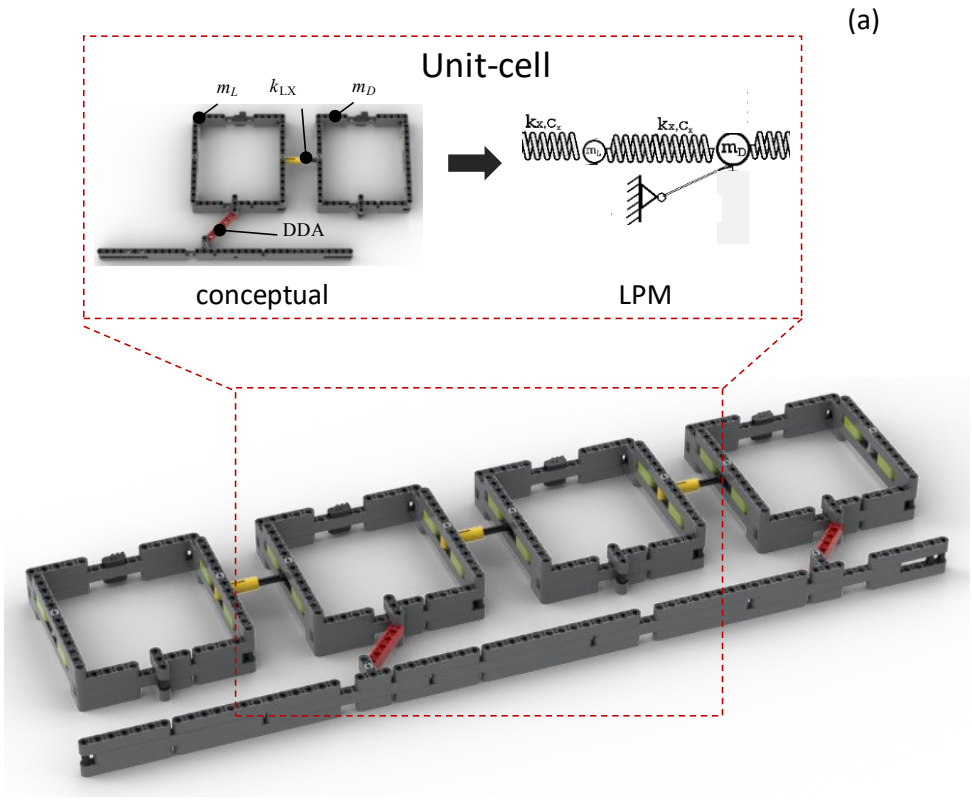

Figure 3: Illustration of the rendered LEGO® DDA enhanced phononic metamaterial design.

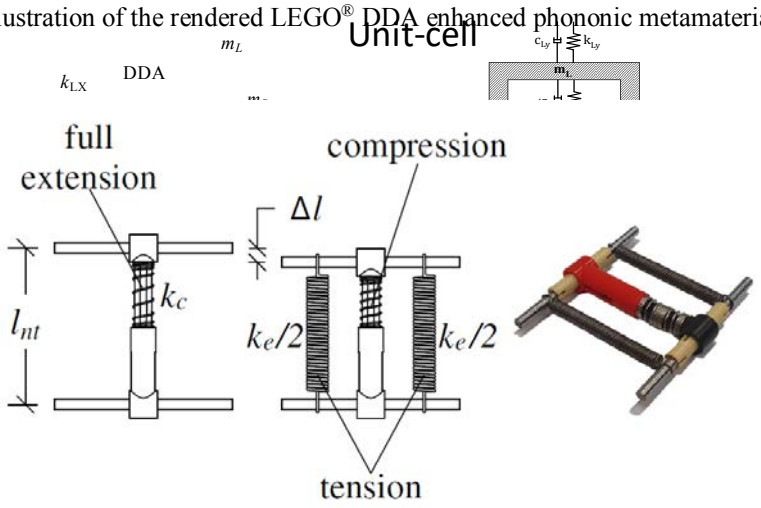

Figure 4: Assembly of the linear stiffness elements at rest: (left) original, (center) modified configuration, (right) physical assembly [17].

The additional components shift the stable equilibrium position backwards by Δl. This allows the system to react equivalently in both the compression and extension states, in contrast to the original configuration, which is at full extension at its equilibrium position. The overall stiffness of the assembly k_n is therefore calculated as:

$$k_n = k_e + k_c \tag{4}$$

Table 1 summarizes the characteristics of the spring assemblies that are used in the models; these are the stiffness value k_n, as well as the individual stiffness of the extension spring (k_e) and compression spring (k_c).

Extension spring k_e [Nm^{-1}]	Compression spring k_c [Nm^{-1}]	Spring Assembly k_N [Nm^{-1}]
80	320	480

Table 1: Stiffness characteristics of the experimentally tested springs.

The mass properties of the individual elements of the phononic metamaterial lattice are tabulated in Table 2. Mass m_L is realized by LEGO ® parts, while mass m_D is adjusted to reach the required weight by installing supplementary steel weights; i.e., $m_D = m_L + m'$, where m' is the additional weight.

Element	Mass (g)
m_L	58
m_D	58
m'	150

Table 2: Mass measurements for the individual parts of the experimental phononic models.

4 DESCRIPTION OF THE SETUP

The configured experimental setup is presented in Figure 5.

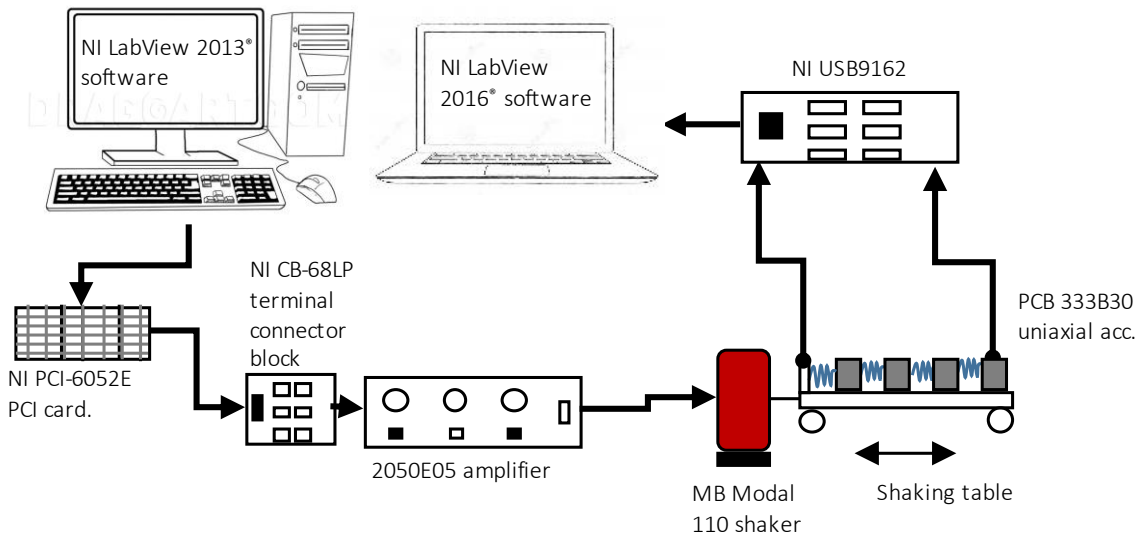

Figure 5: Schematic diagram of the experimental setup.

An MB Modal 110 (MB Dynamics) electrodynamic shaker applies a one-dimensional (1D) horizontal input excitation. A timber board is mounted at the shaker's shaft on one side, to function as a shaking table, while longitudinal guides and bearings provide support, maintain the table in a levelled position, and limit parasitic vertical oscillations. A digital signal generator creates the harmonic sweep and a 2050E05 (modal shop INC) amplifier receives the pro-

duced signal and activates the shaker. Both sinusoidal inputs as well as sine sweeps can be generated by controlling the voltage signal of the shaker. This signal results to a nearly flat spectrum for a given frequency range, thus exciting uniformly the specified range.

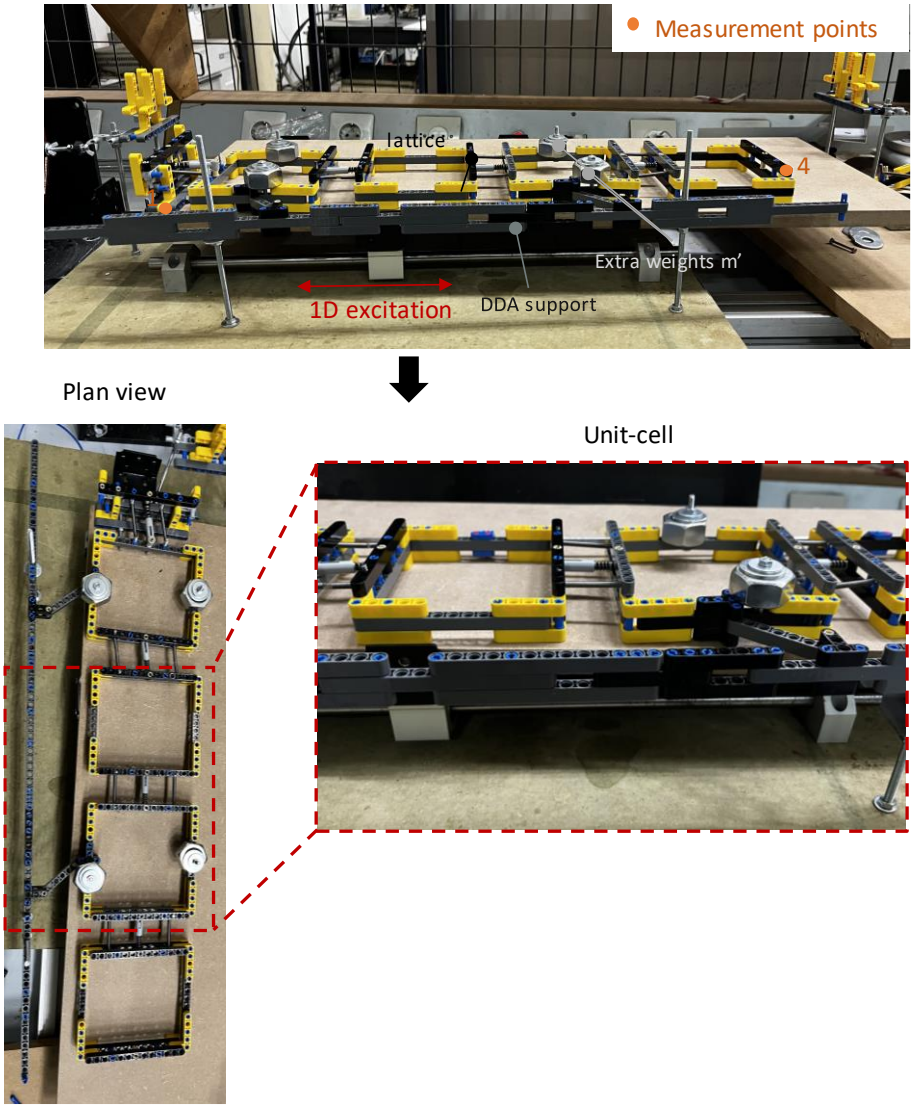

Figure 6: Overview of the LEGO® DDA enhanced phononic structure consisting of four (4) unit-cells.

The metamaterial chain is installed at the shaking table, where longitudinal guides ensure that displacements develop primarily in the desired direction, while lubricant liquid minimizes the effect of friction between the guides and the support. Apart from this minimal inevitable friction, the cells are completely detached from the shaking table. The input is applied to the left end of the chain, where the support of the first cell is mounted to the shacking table, hence creating longitudinal waves to propagate within the lattice.

The dynamic response of the system is measured using uniaxial PCB 333B30 accelerometers with 10.2 $mV/m/s^2$ sensitivity and a sampling frequency of 2 kHz. The measuring locations include the last unit-cell, as well as the shaker input signal. The accelerometers are connected to the computer through an NI USB9162 card. The recording of the measurements is done via the NI LabView 2016® software, while the post-processing is carried out using in-house developed scripts on the MATLAB R2020b® software.

The DDA enhanced lattice is presented in Figure 6. In this case the amplifiers are added to the units with the extra masses m' and an external LEGO® arrangement is erected in front of the shaking table. The links form an angle $\varphi \approx 60°$ with the units and longitudinal guides are added only to those units that are not connected with an amplifier, allowing in this way the others to rotate freely.

5 EXPERIMENTAL RESULTS

This section discusses the obtained experimental results. The tests include inputs of sine-sweep excitation and validation through single-harmonic inputs. The acceleration measurements are carried out with small amplitude excitations to ensure that the metamaterial features a linear elastic behaviour. The experimental wave transmission spectrum is obtained as the ratio between the output and input spectral accelerations $F\left\{\ddot{u}_{fin}^{out} / \ddot{u}_{1}^{in}\right\}$ using the FFT function and the efficiency of each metamaterial device is evaluated upon its attenuation capabilities. The attenuation zone of the tested metamaterial device corresponds to the regions where the ratio of the frequency content between output and input falls below unity and is compared to the analytically predicted bandgaps.

The analysis of the experimental results of the phononic structures begins with the theoretical estimation of the dispersion curves. Figure 7 (a) indicates the frequency range that an attenuation zone is expected from the experimental measurements before and after the addition of the amplifiers. The amplifiers improve the expected bandgap by 60%; the acoustic branch of the dispersion curves is expected to shift from 8.5 to 4.5 Hz. Then, a comparison is carried out in Figure 7(b) between the theoretically estimated dynamic response and the experimentally measured frequency response of the conventional phononic structure (device w/o the DDA mechanism), in order to verify the performance of the experimental setup.

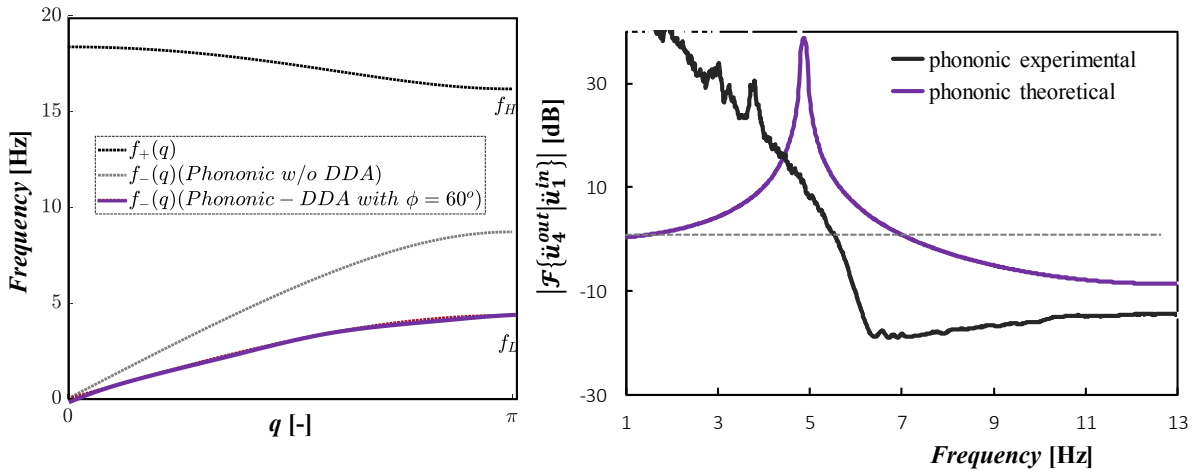

(a) (b)

Figure 7: (a) Expected theoretical dispersion curves of the phononic LEGO® technics assemblies. (b) Comparison between the experimental and analytically estimated frequency response $F\left\{\ddot{u}_4^{out} / \ddot{u}_1^{in}\right\}$ $\mathcal{F}\{\ddot{u}_4^{out}|\ddot{u}_1^{in}\}\mathcal{F}\{\ddot{u}_4^{out}|\ddot{u}_1^{in}\}\mathcal{F}\{\ddot{u}_4^{out}|\ddot{u}_1^{in}\}$ for the four (4) unit-cell chain of the phononic structure.

It is obvious that only the acoustic part of the dispersion relation is explored, as the optical branch corresponds to much higher frequencies which are not studied herein. Therefore, in this low-frequency regime, only the opening frequency of the bandgap is spotted, where for lower values, wave propagation is not prohibited and for higher attenuation is present. Fur-

thermore, it is observed that the two curves show some differences in terms of the opening frequency of the attenuation zone and the resonance peak, yet, the general dynamic performance of the metamaterial is captured; the experimental bandgap due to Bragg scattering is realized. At this point it should be mentioned that a minimal amount of damping ($\zeta = 5\%$) is prescribed at the analytical model, arising from the developed friction between the guides and the units.

Next, for the sake of comparison, the frequency response of the metamaterial device with and without the amplification mechanisms are plotted together. Figure 8 illustrates the experimental dynamic response of the two structures, where the enlargement of the attenuation zone is apparent after the inclusion of the DDA. As discussed, the upper limit of the bandgap could not be measured, nonetheless, an approximate difference of 1.5Hz is observed between the opening theoretical estimated frequencies (demonstrated by the shaded areas) and the experimentally measured ones.

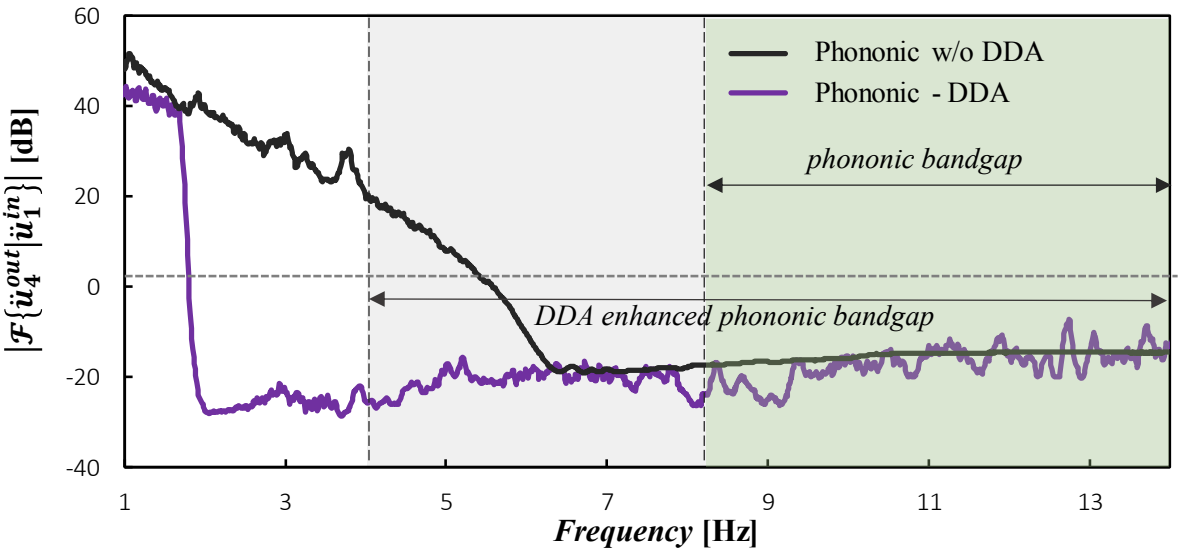

Figure 8: Frequency content of the response of the phononic lattice with and w/o the DDA φ=60° for a four (4) unit-cell lattice. The maximum acceleration of each unit p is denoted as max $\ddot{u}_p^L$.

Overall, the dynamic response of the proposed prototypes verifies the analytically predicted response of the two arrangements, exhibiting the capabilities of the DDA enhanced phononic lattices.

6 CONCLUSIONS

In this paper, the dynamic and filtering properties of a conventional phononic structure and a DDA-enhanced phononic structure were experimentally investigated. The unit blocks of both arrangements consist of LEGO® assemblies connected to each other through spring assemblies comprising compression and extension springs.

Phononic Bragg bandgaps were sought in the very low-frequency regime based on theoretical predictions based on dispersion analysis. The experimental tests proved the existence of these attenuation zones and revealed the opening bandgap frequency. Specifically, the DDA-enhanced structure clearly showed a better response compared to the conventional structure;

the lower bound of the bandgap was shifted to lower frequencies, increasing this way the overall width of the attenuation zone.

It is concluded that the DDA inertial amplification mechanism can be used for enhancing the design of vibration mitigation structures and shock-absorbing materials at various length scales. While this is an initial investigation, validated by a scaled proof-of-concept system, the feasibility of the proposed designs as well as the potential practical limitations should be further studied prior to proceeding to realistic full-scale applications. The practical implementation aspects of the proposed designs for seismic protection of structures, energy harvesting, or acoustic absorption are topics of interest for future examination.

ACKNOWLEDGMENTS

M. Kalderon, A. Mantakas & K.A. Chondrogiannis would like to acknowledge the financial support provided by the European Union's Horizon 2020 research and innovation program under the Marie Sklodowska-Curie grant (Grant Agreement No. INSPIRE-813424).

REFERENCES

[1] C. Yilmaz, G.M. Hulbert, N. Kikuchi, Phononic band gaps induced by inertial amplification in periodic media, *Phys. Rev. B.* **76** (2007) 54309..

[2] O. Yuksel, C. Yilmaz, Shape optimization of phononic band gap structures incorporating inertial amplification mechanisms, *J. Sound Vib.* **355** (2015) 232–245.

[3] C. Yilmaz, G.M. Hulbert, Theory of phononic gaps induced by inertial amplification in finite structures, Phys. Lett. Sect. A Gen. At. Solid State Phys. **374** (2010) 3576–3584.

[4] G. Acar, C. Yilmaz, Experimental and numerical evidence for the existence of wide and deep phononic gaps induced by inertial amplification in two-dimensional solid structures, *J. Sound Vib.* **332** (2013) 6389–6404.

[5] S. Taniker, C. Yilmaz, Generating ultra wide vibration stop bands by a novel inertial amplification mechanism topology with flexure hinges, *Int. J. Solids Struct.* 106–107 (2017) 129–138.

[6] Y. Mi, X. Yu, Sound transmission of acoustic metamaterial beams with periodic inertial amplification mechanisms, *J. Sound Vib.* **499** (2021) 116009. https://doi.org/https://doi.org/10.1016/j.jsv.2021.116009.

[7] Y. Zeng, L. Cao, S. Wan, T. Guo, Y.-F. Wang, Q.-J. Du, B. Assouar, Y.-S. Wang, Seismic metamaterials: Generating low-frequency bandgaps induced by inertial amplification, *Int. J. Mech. Sci.* **221** (2022) 107224.

[8] S. Muhammad, S. Wang, F. Li, C. Zhang, Bandgap enhancement of periodic nonuniform metamaterial beams with inertial amplification mechanisms, *J. Vib. Control.* **26** (2020) 1309–1318.

[9] M. Mazzotti, A. Foehr, O.R. Bilal, A. Bergamini, F. Bosia, C. Daraio, N.M. Pugno, M. Miniaci, Bio-inspired non self-similar hierarchical elastic metamaterials, *Int. J. Mech. Sci.* **241** (2023) 107915.

[10] Q. Lin, J. Zhou, K. Wang, D. Xu, G. Wen, Q. Wang, Three-dimensional quasi-zero-

stiffness metamaterial for low-frequency and wide complete band gap, *Compos. Struct.* **307** (2023) 116656.

[11] J. Zhou, H. Pan, C. Cai, D. Xu, Tunable ultralow frequency wave attenuations in one-dimensional quasi-zero-stiffness metamaterial, I*nt. J. Mech. Mater. Des.* **17** (2021) 285–300.

[12] S. Taniker, C. Yilmaz, Generating ultra wide vibration stop bands by a novel inertial amplification mechanism topology with flexure hinges, *Int. J. Solids Struct.* 106–107 (2017) 129–138.

[13] S. Taniker, C. Yilmaz, Design, analysis and experimental investigation of three-dimensional structures with inertial amplification induced vibration stop bands, *Int. J. Solids Struct.* 72 (2015) 88–97.

[14] O. Yuksel, C. Yilmaz, Realization of an ultrawide stop band in a 2-D elastic metamaterial with topologically optimized inertial amplification mechanisms, *Int. J. Solids Struct.* **203** (2020) 138–150.

[15] A. Bergamini, M. Miniaci, T. Delpero, D. Tallarico, B. Van Damme, G. Hannema, I. Leibacher, A. Zemp, Tacticity in chiral phononic crystals, *Nat. Commun.* **10** (2019) 4525.

[16] R. Zaccherini, A. Colombi, A. Palermo, H.R. Thomsen, E.N. Chatzi, Stress-optimized inertial amplified metastructure with opposite chirality for vibration attenuation, *arXiv*, (2021).

[17] K.A. Chondrogiannis, A. Colombi, V. Dertimanis, E. Chatzi, Computational Verification and Experimental Validation of the Vibration-Attenuation Properties of a Geometrically Nonlinear Metamaterial Design, *Phys. Rev. Appl.* **17** (2022) 54023.

[18] M. Kalderon, A. Paradeisiotis, I.A. Antoniadis, A Phononic Metamaterial Incorporating Directional Amplification for Low Frequency Isolation, *Int. Conf. Nat. Hazards Infrastruct. (ICONHIC)*, Athens, Greece, July 5-7, 2022.

[19] M. Kalderon, A. Mantakas, I. Antoniadis, Dynamic Modelling and Experimental Testing of a Dynamic Directional Amplification Mechanism for Vibration Mitigation, *J. Vib. Eng. Technol.* (2023).

[20] M. Kalderon, A. Paradeisiotis, I. Antoniadis, 2D Dynamic Directional Amplification (DDA) in Phononic Metamaterials, *Materials (Basel)*. **14** (2021).

[21] M. Kalderon, A. Mantakas, A. Paradeisiotis, I. Antoniadis, E.J. Sapountzakis, Locally resonant metamaterials utilizing dynamic directional amplification: An application for seismic mitigation, *Appl. Math. Model.* **110** (2022) 1–16.

[22] P. Martakis, G. Aguzzi, V.K. Dertimanis, E.N. Chatzi, A. Colombi, Nonlinear periodic foundations for seismic protection: Practical design, realistic evaluation and stability considerations, *Soil Dyn. Earthq. Eng.* **150** (2021) 106934.

[23] A. Colombi, R. Zaccherini, G. Aguzzi, A. Palermo, E. Chatzi, Mitigation of seismic waves: Metabarriers and metafoundations bench tested, *J. Sound Vib.* **485** (2020)